A Low-Cost Experimental Ultra-Wideband Positioning System

Jens Schroeder, Stefan Galler, and Kyandoghere Kyamakya

A Low-Cost Experimental Ultra-Wideband Positioning System

Jens Schroeder, Stefan Galler, and Kyandoghere Kyamakya

Abstract—**In this paper we report on the architecture and implementation status of a low-cost experimental Ultra-Wideband (UWB) local positioning system, designed to enable practical evaluations of UWB based positioning concepts. The mobile devices use the avalanche effect of transistors for simple generation of bi-phase pulses and are TDMA multi-user capable. After high-speed analog-to-digital conversion, the receiver is implemented in software and employs direct cross-correlation with maximum detection to localize the mobile unit via Time-Difference-Of-Arrival (TDOA) algorithms. One direct solution and one nonlinear optimization approach are implemented. First measurement results are presented, showing accuracy in the order of decimeters.**

Index Terms—**Ultra-Wideband, localization, TDOA, pulse generator**

I. Introduction

Ultra-Wideband technology is regarded by many as one of the future key technologies in communications and positioning. Even though the basic principles of UWB have been studied for decades, there is still a great demand for research, especially in the field of precise local positioning. Techniques have to be further developed to cope with for example varying line of sight (LOS) / non line of sight (NLOS) or severe multipath conditions. In order to verify analytical and simulation results with real-world measurements, the need for experimental UWB systems arises. However, since commercially available Ultra-Wideband localization systems do not allow access to neither the physical layer nor later processing stages, we have developed a low-cost experimental UWB positioning system, involving some of the ideas of the work described in [1, 2]. The term "low cost" in this context corresponds to the possible deployment of a large number of mobile units, which can be assembled easily, cost-efficiently, and without high technical complexity. In comparison, the base station design using high-speed analog to digital converters cannot be regarded as low-cost. However, this system design offers the ease to evaluate different receiver architectures in software, and recent hardware developments such as those described in [3, 4] seem to be promising for the near future.

This paper describes the current state of our UWB positioning system, the architecture of which will be described in section II. Section III deals with the TDOA localization methods that have been used to estimate the mobile unit's position. Section IV presents and discusses the measurements which have been carried out in a laboratory room at IANT.

Manuscript received March 31, 2005. This work was supported in part by the competence center Niccimon (Lower Saxony, Germany), the DFG (German Research Foundation) under Grant KIOP, and the Minna-James-Heinemann Foundation.

J. Schroeder, S. Galler, and K. Kyamakya are with the Institute of Communications Engineering (IANT), Location Based Services and Systems Group, University of Hannover, Hannover, Germany (phone: +49(511)762-2814; fax: +49(511)762-3030; e-mail: (jens.schroeder, galler, kyandogh)@ant.uni-hannover.de).

II. System Architecture

The system consists of the infrastructure components (a standard PC, a high-speed sampling oscilloscope, and a triggering unit) and a possible multiple number of mobile devices presented in Fig. 1.

We have chosen TDMA as multiple access scheme since it suits best to our needs. FDMA in contrast, would lead to a more complex pulse generation, hence, higher costs. CDMA with concurrent position estimation, however, would complicate anticipated analysis and exploitation of channel properties.

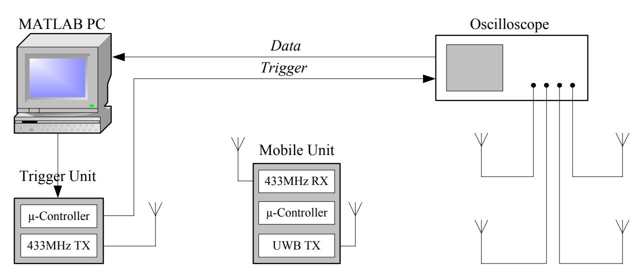

Fig. 1. Architecture of the low-cost experimental UWB positioning system.

A. The infrastructure components

Central controller of the positioning system is a PC running Matlab. The PC connects to the sampling oscilloscope via Ethernet and to the triggering unit via RS232. The triggering unit consists of a standard 433 MHz transmitter and an Atmel ATMEGA16 microcontroller. The 433 MHz link was chosen, since it allows a simple and cost-effective implementation of a

0-7803-9398-8/05/$20.00 ©2005 IEEE

TDMA scheme. The tasks of this unit are to send activation IDs to the mobile device via the 433 MHz link and to trigger the sampling oscilloscope by wire. As a sampling oscilloscope, we use an Agilent infinium 54855A running at a sample rate of F_S=5 *GS/s* with a memory depth of 262.144 samples per channel. When triggered, the oscilloscope simultaneously captures signals received by the four antennas connected to its inputs.

Commercially available Arc Freedom antennas are used, which feature acceptable radiation and reception characteristics in the utilized frequency range for a tolerable price [5]. The horizontal beamwidth is described as 360° with a gain of 3 dBi.

To calculate the mobile devices' positions, all measurement data are transferred from the oscilloscope to the PC. Fig. 2 shows the direct cross-correlation receiver structure implemented in Matlab, considering as example channel 1 and channel 2:

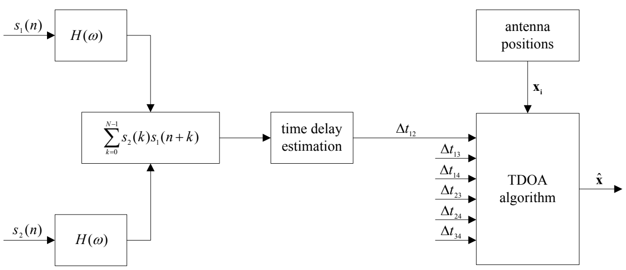

Fig. 2. Direct cross-correlation receiver implementation in Matlab.

Before cross-correlation, each channel $s_i(n), 1 \le i \le 4$ is pre-filtered with $H(\omega)$ to suppress interference. In the current configuration, $H(\omega)$ is implemented as a simple bandpass filter with passband frequencies from 1.1 to 1.7 GHz, since only low interference occurs in this band. However, the architecture leaves the opportunity for implementing interference suppression methods with higher complexity, offering the possibility to exploit the complete spectrum of the pulses.

The time delay differences Δt_{12}, Δt_{13}, Δt_{14}, Δt_{23}, Δt_{24} and Δt_{34} are estimated by a maximum search and fed with the antenna positions $\mathbf{x_i}$ into a TDOA localization algorithm to compute the mobile device's position estimate $\hat{\mathbf{x}}$.

B. The mobile devices

Each mobile device comprises a 433 MHz receiver, an Atmel ATMEGA16 microcontroller and an UWB bi-phase pulse generator along with required power circuitry and batteries (Fig. 3). The same type of antennas as at the infrastructure side is used. Based on a simple mono-phase pulser described in [6], the design has been extended to be capable of using the avalanche effect of two transistors, resulting in a bi-phase pulse generator (Fig. 4).

When the mobile device is activated, pulses are triggered at a rate of 3.2 MHz by the microcontroller according to a pre-stored pseudo random code sequence of length 128. This code sequence was generated using computer simulations to achieve good autocorrelation properties. Since the capacitors *C1* or *C3* need to be fully charged for the respective transistor to emit a pulse, the design of the pulse generator does not allow for a pulse repetition frequency higher than 3.2 MHz (quantized by the 16 MHz clock of the microcontroller).

Fig. 3. The mobile device

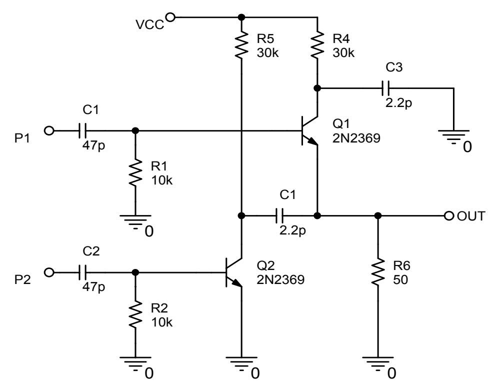

Fig. 4. Circuit diagram of the bi-phase pulse generator using the avalanche effect of two NPN-transistors.

C. System operation

The system operation according to a TDMA scheme ensures multi-user capability and is organized as follows: The Matlab PC initiates a measuring procedure by sending an 8 Bit mobile device ID to the triggering unit. The triggering unit's microprocessor forms a Manchester coded 8 Bit signal to be transmitted to activate the selected mobile device. After sending the activation ID, the sampling oscilloscope is triggered to start filling up its internal memory. When the activation ID is received by a mobile unit, its microcontroller compares the received ID with its own stored ID. In case the IDs are different, the mobile device goes back to listening mode. In case the IDs match, the microcontroller triggers the UWB pulse generator with the pre-stored pseudo random code sequence. The internal memory of the sampling oscilloscope records the transmitted pulse train and the set of measurement data is transmitted to the Matlab PC. The measurement procedure is completed with the computation of the mobile device's position.

III. TDOA Localization Algorithms

For our setup the simplest localization method is Time-Difference-Of-Arrival (TDOA), since we have an inherent synchronization of all base stations[1] at the oscilloscope. Therefore, we do not need to rely on synchronization of mobile unit and base stations as required for Time-Of-Arrival (TOA). However, since a TDOA-based positioning system does not measure absolute time, but instead time differences, signal waveforms received at at least four base stations must be recorded and crosscorrelated with each other for 3D positioning. Time differences are obtained by taking the argument of the peak of the crosscorrelation functions between two respective base stations and are regarded as the TDOA estimate.

Mathematically, this can be formulated as follows: If we denote $s_i(t)$ the received time-domain signal of length T at base station i, and $s_j(t)$ the received signal at base station j, the TDOA estimate Δt_{ij} between base station i and j can be written as

$$\Delta t_{ij} = t_i - t_j = \arg\max_{\tau} \int_{-T/2}^{T/2} s_j(t) s_i(t+\tau)\, dt \,, \; 1 \le i < j \le N \,, \tag{1}$$

where t_i and t_j are the absolute times of arrival at base station i and j, respectively, and N represents the number of base stations.

The TDOA estimates are converted to range differences Δd_{ij} by multiplying by the speed of light c:

$$\Delta d_{ij} = c \cdot \Delta t_{ij} = c(t_i - t_j) = d_i - d_j \,. \tag{2}$$

In a Cartesian coordinate frame the Euclidian distance d_i between mobile unit and base station i is given by

$$d_i = \left\| \mathbf{x} - \mathbf{x_i} \right\| = \sqrt{(x-x_i)^2 + (y-y_i)^2 + (z-z_i)^2} \,, \tag{3}$$

with the mobile unit's position $\mathbf{x} = [x, y, z]^T$, the i[th] base station position $\mathbf{x_i} = [x_i, y_i, z_i]^T$, and $\|\ldots\|$ denoting the L^2 norm. Substituting the distances d_i of (3) into the range difference formula (2) yields

$$c \cdot \Delta t_{ij} = \left\| \mathbf{x} - \mathbf{x_i} \right\| - \left\| \mathbf{x} - \mathbf{x_j} \right\| , \; 1 \le i < j \le N \,. \tag{4}$$

The indices (i,j) account for all K permutations of pairs of base stations, resulting in a set of

$$K = \binom{N}{2} \tag{5}$$

so called pseudo-range equations. Hence, the general problem is to solve the non-linear system of K (usually over-determined) equations for the mobile unit's position $\mathbf{x}$, given the base stations' positions $\mathbf{x_i}$ and the TDOA measurements Δt_{ij}. The intersection of these hyperbolas corresponds to the position of the mobile unit, if the TDOA measurements Δt_{ij} are exact.

Therefore, one way to find a position estimate from TDOA measurements is the direct solution of the set of pseudo-range equations. Various algorithms exist, e.g. [7-9], with analyzed solutions concerning uniqueness and existence under measurement errors and base station geometry [10]. Here, we used Bancroft's algorithm for solving the hyperbolic localization problem, which gives a direct solution valid for 3D positioning with at least four base stations and is easy to implement.

To cope with lesser performance of the direct solution when the errors of the TDOA estimates increase, algorithms from nonlinear optimization theory have been found to be more appropriate for position estimation [11, 12]. The objective function can be defined as the sum of nonlinear least-square range difference errors, derived from the pseudo-range equations (4):

$$F(\mathbf{x}) = \sum_{i=1}^{N-1} \sum_{j=i+1}^{N} f_{ij}^2(\mathbf{x}) \,, \text{ with} \tag{6}$$

$$f_{ij}(\mathbf{x}) = c \cdot \Delta t_{ij} - \left(\left\| \mathbf{x} - \mathbf{x_i} \right\| - \left\| \mathbf{x} - \mathbf{x_j} \right\| \right) . \tag{7}$$

Now, the nonlinear least-square estimate can be found at the minimum of the objective function:

$$\hat{\mathbf{x}} = \arg\min_{\mathbf{x}} F(\mathbf{x}) \,. \tag{8}$$

Various optimization methods exist to minimize the objective function resulting in an estimate $\hat{\mathbf{x}}$ for the mobile unit's position. Currently, we use Matlab's implementation of the quasi-Newton algorithm with the steepest descent option, which has been found to perform best in our scenario. The initial position has been chosen as the geometrical center of the room. It seems, however, that the z-coordinate estimate is dependent on the initial z-coordinate, which is considered to be due to base station geometry. Further investigations have to elaborate this issue and examine other optimization methods and varying geometry.

IV. Measurement Results

To analyze system characteristics, pulse train transmission via the antennas was recorded in an anechoic chamber. Afterwards, two sets of measurements were conducted in a laboratory room in addition to prior calibration measurements to investigate real world behavior of the positioning system.

A. Anechoic chamber

Fig. 5 depicts a positive pulse transmitted via cable and via antennas in an anechoic chamber, respectively recorded with the oscilloscope. The double differential behavior of the two antennas can be observed. Pulse-durations are in the order of sub-nanoseconds, corresponding to a measured bandwidth of

[1] A base station is regarded as one antenna of the infrastructure component in conjunction with one channel of the sampling oscilloscope.

approximately 1.6 GHz. Assuming a fully balanced system, pulse peak power according to pulse peak amplitude of 7.3 V can be estimated to be 30 dBm into a 50 Ω load. Average pulse power at pulse repetition frequency can be estimated to be 0 dBm into a 50 Ω load.

Preliminary analysis of the pulse trains resulted in two drawbacks concerning timing. First, the low-cost clock of the microcontroller results in high jitter of the pulse position (ca. 600 ps RMS for positive pulses, ca. 420 ps RMS for negative pulses). This makes it impossible to use template or transmitted reference correlation at the receiver side [13], which has been confirmed by the non-detectability of template correlation peaks evaluated with our measurements. However, the jitter causes spectrum smoothing as a positive consequence. Second, the pulse generator shows a timing offset of positive and negative pulse positions of about 30 ns. Since the sent random sequence is known, the latter could be compensated for. Yet the first effect cannot be revoked.

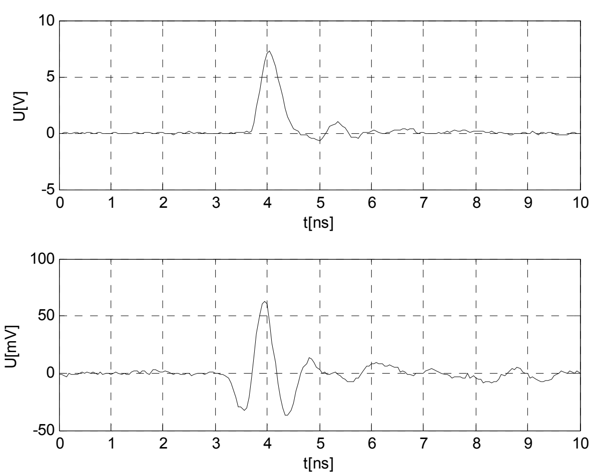

Fig. 5. Top: measured positive pulse via cable directly connected to oscilloscope. Bottom: transmitted pulse via antennas in an anechoic chamber.

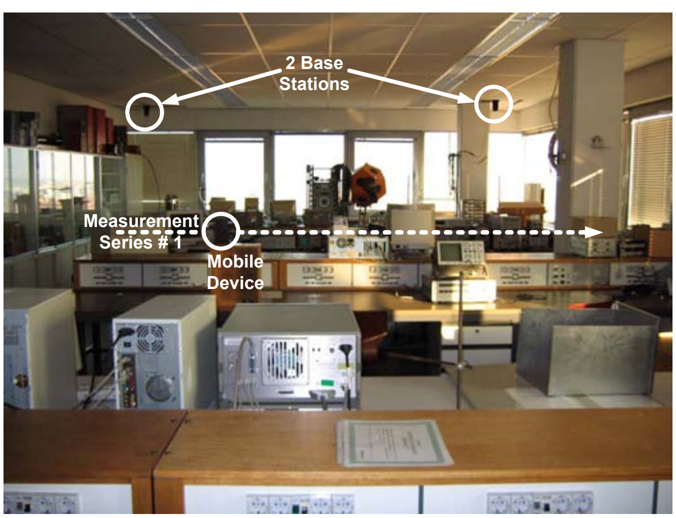

Fig. 6. Laboratory room at IANT showing the mobile device and two base stations.

B. Laboratory room

Real world measurements were taken in a laboratory room at the IANT (Fig. 6). All real positions of the mobile device and infrastructure were determined using a Zeiss Elta C3 tachymeter. Because of the indoor environment and the presence of many metallic objects, the channels were subject to severe multipath. However, at all positions of the mobile device, LOS paths were present.

The mobile unit was moved in 5 cm steps along a 3 m line parallel to the y-axis of the coordinate system on two different heights (referred to as *measurement series # 1* and *# 2*). In addition, 100 measurements were taken at a single location on *measurement series # 1* for calibrating range offsets due to the not exactly known cable lengths to the antennas and further system offsets. A nonlinear least square error approach was taken to calculate the offsets.

Fig. 7 shows the estimated range differences of *measurement series # 1* after calibration in comparison to the real differences. Although the general trend seems to be correct, several outliers can be observed, based on misdetection of the direct difference path.

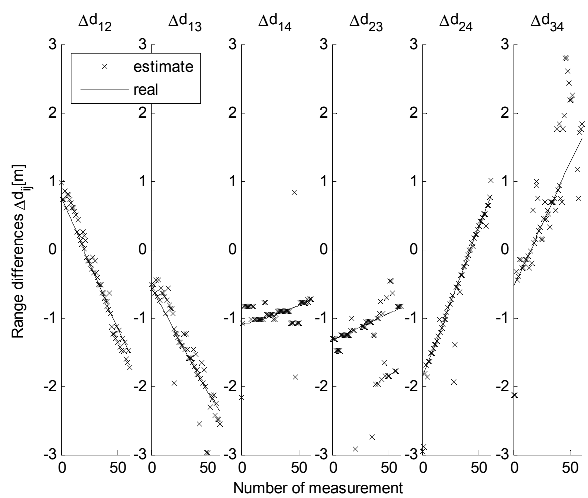

Fig. 7. Range differences among all 4 antennas with the straight line showing the real and the crosses showing the estimated range differences of all 60 measurements of *measurement series # 1*.

C. Accuracy performance

The performance of the system using the two TDOA algorithms with *N=4* base stations is assessed using the position errors of each measurement regarded as the Euclidean distance between the position estimate and the real position, i.e. $e^{<l>} = \|\hat{\mathbf{x}} - \mathbf{x}\|$. Fig. 8 shows that the quasi-Newton algorithm leads to superior results compared to the direct solution. As additional performance metrics serve the root mean square (RMS) error $e_{RMS}^{<P>}$, the arimetic mean μ, the standard deviation σ and an estimate of the cumulative distribution function $cdf(e^{<l>})$. The RMS error of P measurements is defined as [14]

$$e_{RMS}^{<P>} = \sqrt{\frac{\sum_{l=1}^{P} e_l^{<1>^2}}{P}} \,. \quad (3)$$

Table I shows the performance metrics of the two measurement series with the quasi-Newton algorithm. Fig. 9 depicts the cumulative distribution function of *measurement series # 1*.

The accuracy of these first measurements is in the order of reported accuracies of similar experiments in literature [2, 12]. Since our measurements are raw measurements without any exploitation of channel characteristics (e.g. intelligent time difference delay estimation), or postprocessing techniques (e.g. Kalman filtering on position estimates) there is potential for improving accuracy.

TABLE I
ACCURACY PERFORMANCE

Metric	Measurement series # 1	Measurement series # 2
$e_{RMS}^{<P>}$	58,1 cm	73,5 cm
μ	39,7 cm	49,3 cm
σ	42,7 cm	55,1 cm

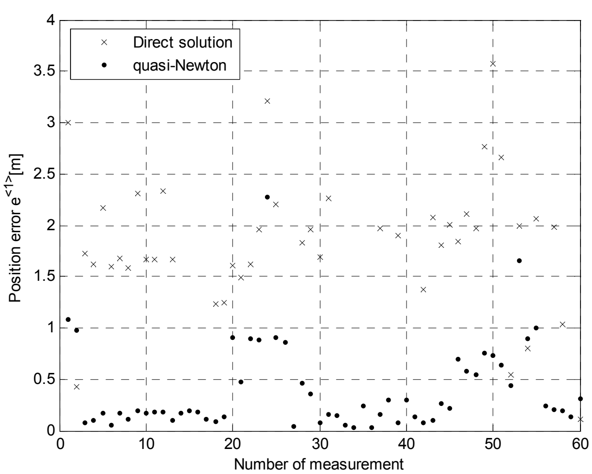

Fig. 8. Position error $e^{<1>}$ of all 60 measurements of *measurement series # 1* using the direct solution and the quasi-Newton approach to estimate the position.

V. CONCLUSION

The architecture, implementation, and measurement results of a low-cost Ultra-Wideband positioning system have been described. The current setup and choice of algorithms demonstrates the functionality of the system, with accuracy in the order of decimeters in a real world laboratory room.

The system now offers the possibility to verify analytical and simulative research on the improvement of accuracy and robustness of UWB localization. Future study activities will include methods for LOS/NLOS distinction and respectively NLOS compensation, multipath detection, and interference cancellation as well as more sophisticated algorithms for time delay and TDOA position estimation and tracking.

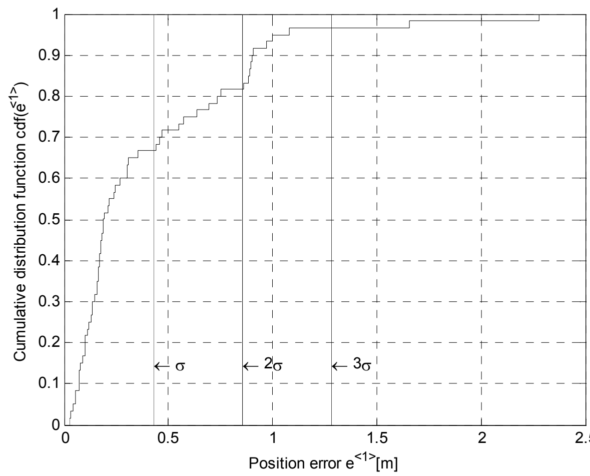

Fig. 9. Estimated cumulative distribution function of position error $e^{<1>}$ of *measurement series # 1*. The vertical lines represent the first, second and third multiple of standard deviation σ.

ACKNOWLEDGMENT

The authors would like to thank the German Regulatory Authority for Telecommunications and Post (RegTP) and the Institute of Electromagnetic Theory and RF Technology (HFT) of the University of Hannover for providing us with digital sampling oscilloscopes and an anechoic chamber.

REFERENCES

[1] J. C. Adams, W. Gregorwich, L. Capots, and D. Liccardo, "Ultra-wideband for navigation and communications," presented at Aerospace Conference, 2001, IEEE Proceedings., 2001.

[2] D. P. Young, C. M. Keller, D. W. Bliss, and K. W. Forsythe, "Ultra-wideband (UWB) transmitter location using time difference of arrival (TDOA) techniques," presented at Signals, Systems & Computers, 2003 The Thrity-Seventh Asilomar Conference on, 2003.

[3] C. Paulus, H.-M. Blüthgen, M. Löw, E. Sicheneder, N. Brüls, A. Courtois, M. Tiebout, and R. Thewes, "A 4GS/s 6b Flash ADC in 0.13µm CMOS," presented at 2004 Symposium on VLSI Circuits, Honolulu, USA, 2004.

[4] M. Tüchler, V. Schwarz, and A. Huber, "Accuracy of an UWB localization system based on a CMOS chip," presented at Joint 2nd Workshop on Positioning, Navigation and Communication 2005 (WPNC'05) & 1st Ultra-Wideband Expert Talk 2005 (UET'05), Hanover, Germany, 2005.

[5] ARC Wireless Solutions Inc., "ARC Freedom Antenna," Wheat Ridge, Colorado, USA www.antennas.com/arcproduct.html.

[6] S. P. Lohmeier, R. Rajaraman, and V. C. Ramasami, "Development of an ultra-wideband radar system for vehicle detection at railway crossings," presented at Ultra Wideband Systems and Technologies, 2002. Digest of Papers. 2002 IEEE Conference on, 2002.

[7] B. T. Fang, "Simple solutions for hyperbolic and related position fixes, "*Aerospace and Electronic Systems, IEEE Transactions on*, vol. 26, pp. 748-753, 1990.

[8] S. Bancroft, "An Algebraic Solution of the GPS Equations, "*IEEE Transactions on Aerospace and Electronic Systems*, vol. AES-21, pp. 56-59, 1985.

[9] Y. T. Chan and K. C. Ho, "A simple and efficient estimator for hyperbolic location, "*Signal Processing, IEEE Transactions on [see also Acoustics, Speech, and Signal Processing, IEEE Transactions on]*, vol. 42, pp. 1905-1915, 1994.

[10] J. S. Abel and J. W. Chaffee, "Existence and uniqueness of GPS solutions, "*Aerospace and Electronic Systems, IEEE Transactions on*, vol. 27, pp. 952-956, 1991.

[11] K. Yu and I. Oppermann, "Performance of UWB position estimation based on time-of-arrival measurements," presented at Ultra Wideband Systems, 2004. Joint with Conference on Ultrawideband Systems and Technologies. Joint UWBST & IWUWBS. 2004 International Workshop on, 2004.

[12] R. J. Fontana, E. Richley, and J. Barney, "Commercialization of an ultra wideband precision asset location system," presented at Ultra Wideband Systems and Technologies, 2003 IEEE Conference on, 2003.

[13] I. Guvenc and H. Arslan, "Performance evaluation of UWB systems in the presence of timing jitter," presented at Ultra Wideband Systems and Technologies, 2003 IEEE Conference on, 2003.

[14] C. R. Drane and C. Rizos, *Positioning systems in intelligent transportation systems*, Boston [u.a.]: Artech House, 1998, pp. 26-29.